Electronic Supporting Information

belonging to

Dinuclear ruthenium complexes containing a new ditopic phthalazin-bis(triazole) ligand that promotes metal–metal interactions

Joan Aguiló,[a,b,c] Atena Naeimi,[a] Roger Bofill,[a] Helge Mueller-Bunz,[c] Antoni Llobet,[a,b] Lluís Escriche,*[a] Xavier Sala,*[a] and Martin Albrecht*[c]

Figure S1. 1D and 2D NMR spectra (500 MHz, 298 K, $CDCl_3$) for **1**: (a) **1** schematic representation, ^{1}H NMR and zoom of the aromatic region (inset), (b) COSY, (c) ^{13}C-{^{1}H}-NMR, (d) HSQC-NMR (aromatic region), (e) HMBC-NMR (aromatic region).

a)

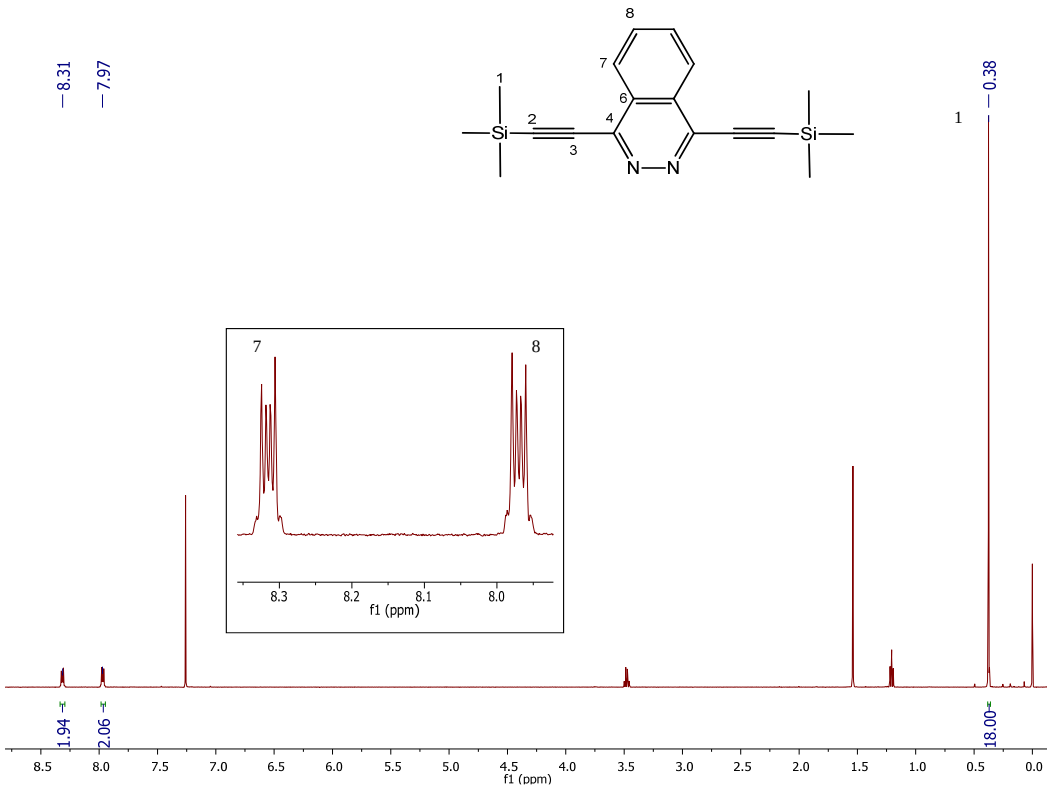

b)

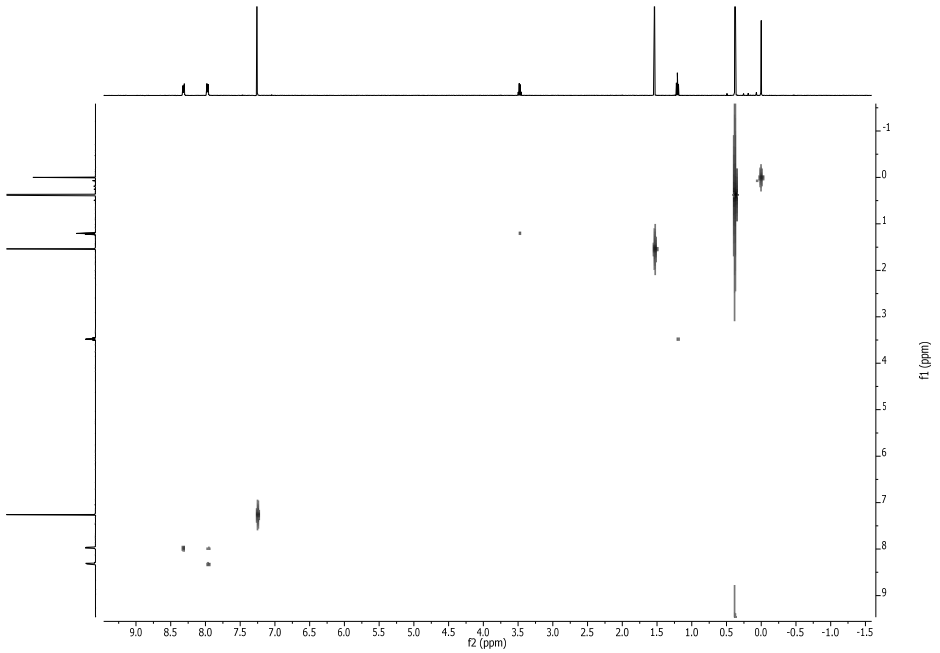

c)

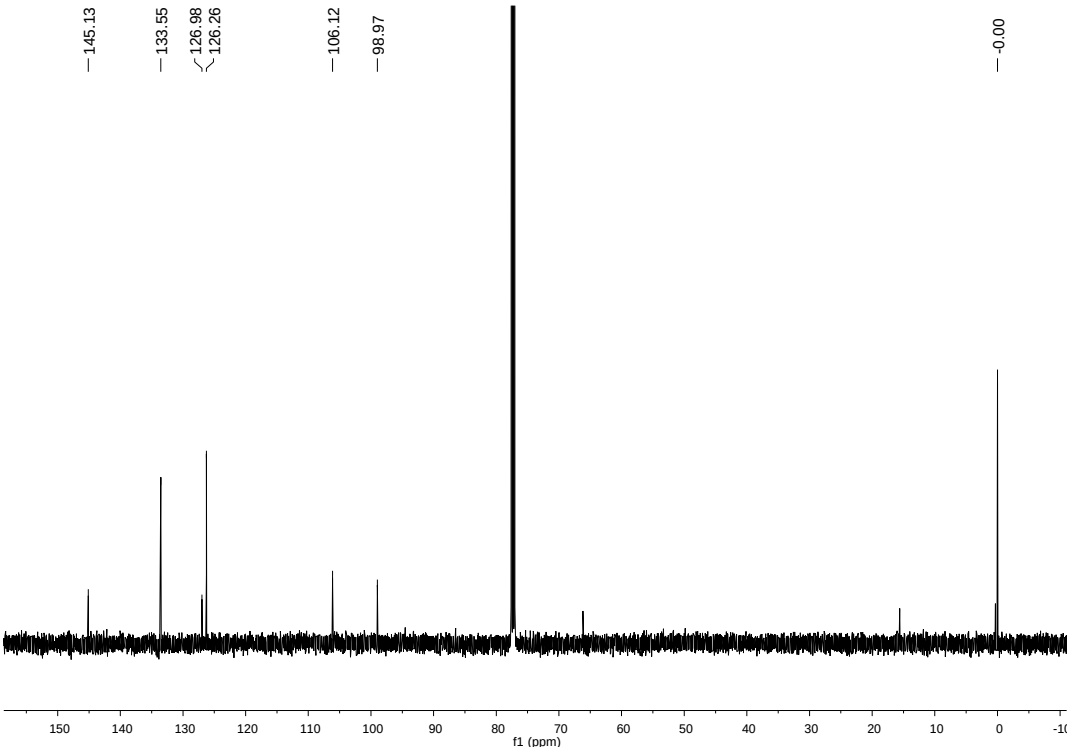

d)

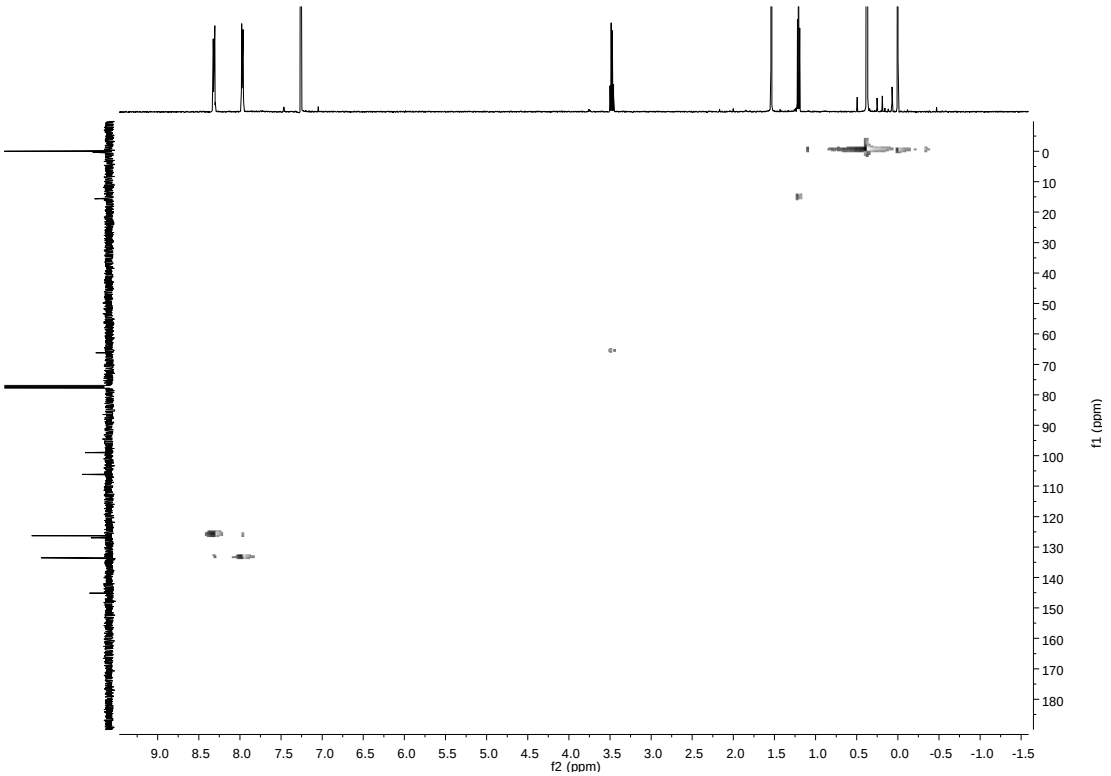

e)

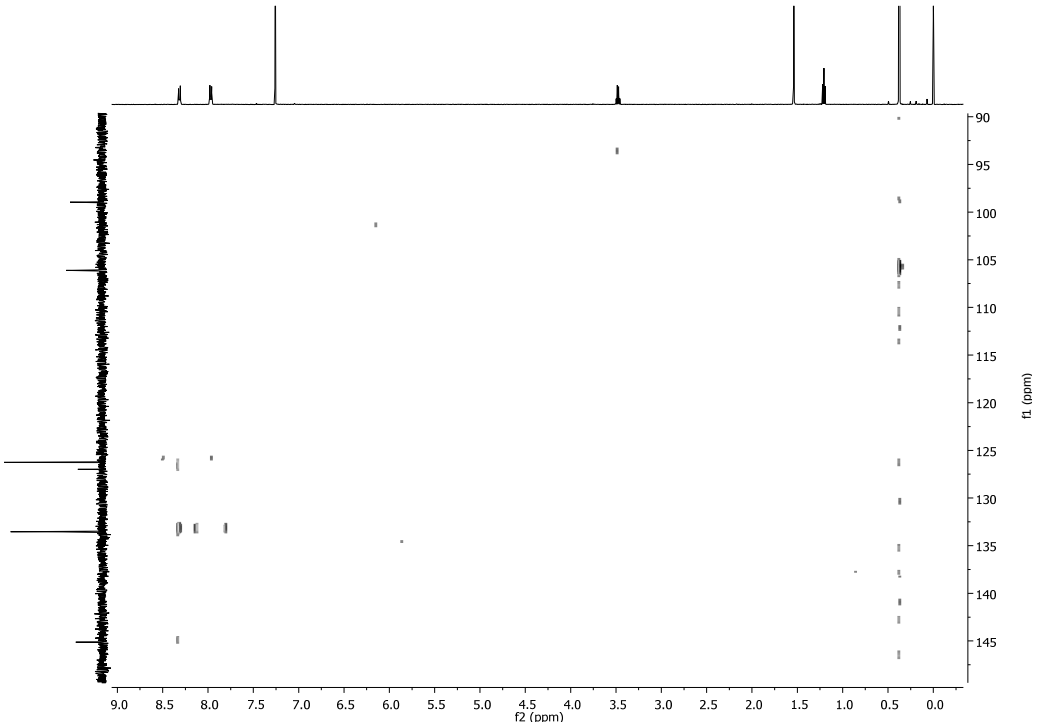

Figure S2. ESI-MS spectrum of **1** recorded in MeOH.

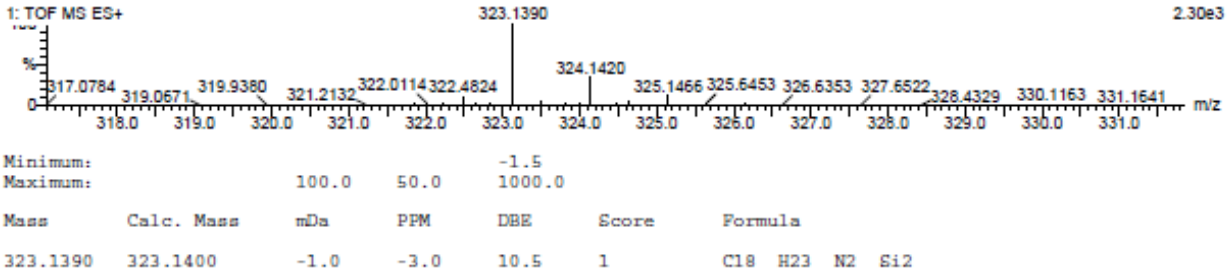

Minimum:				-1.5		
Maximum:		100.0	50.0	1000.0		
Mass	Calc. Mass	mDa	PPM	DBE	Score	Formula
323.1390	323.1400	-1.0	-3.0	10.5	1	C18 H23 N2 Si2

Figure S3. 1D and 2D NMR spectra (500 MHz, 298 K, $CDCl_3$) for **2**: (a) **2** schematic representation and ^{1}H NMR, (b) COSY, (c) ^{13}C-{^{1}H}-NMR, (d) HSQC-NMR (aromatic region).

a)

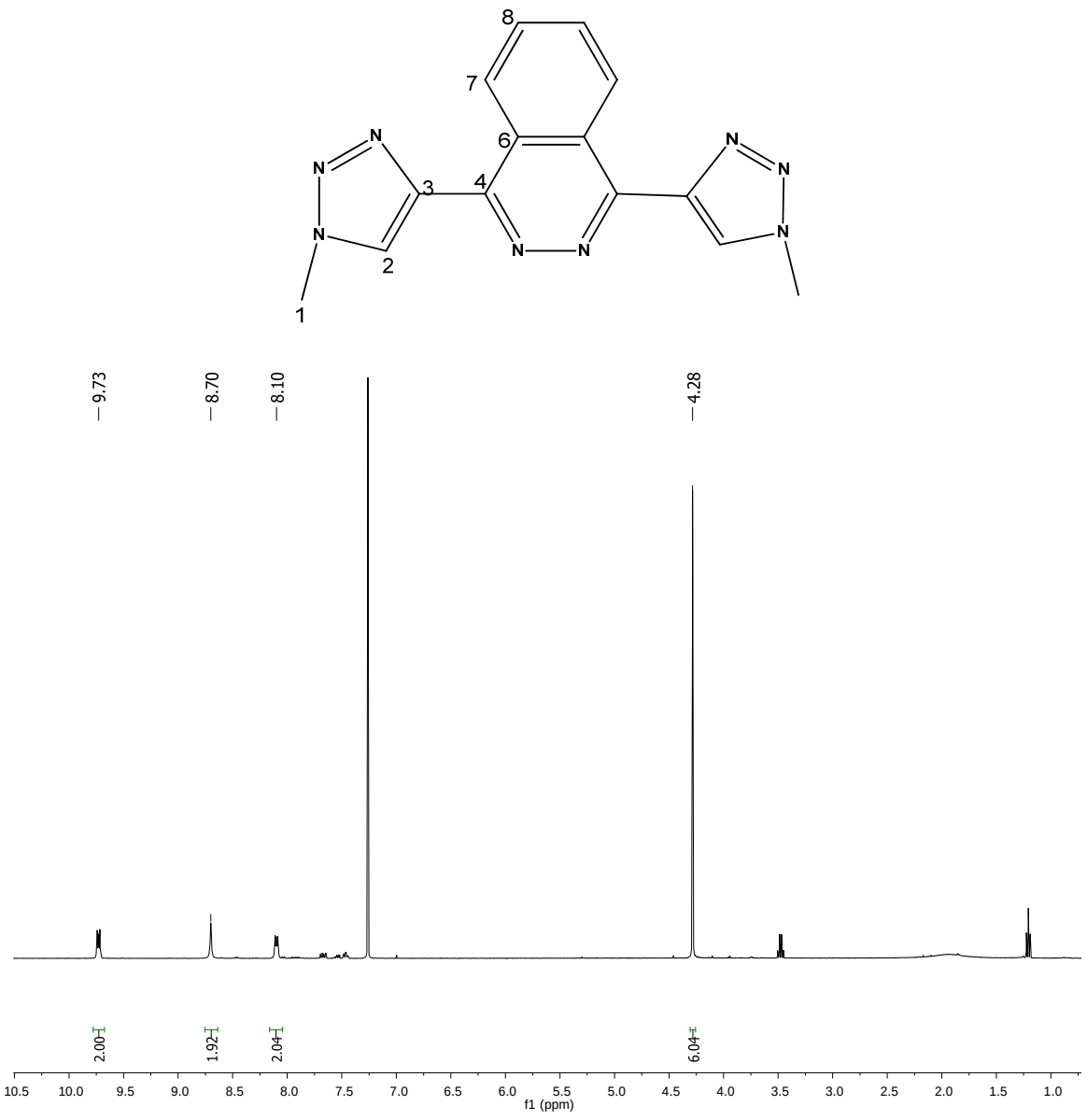

b)

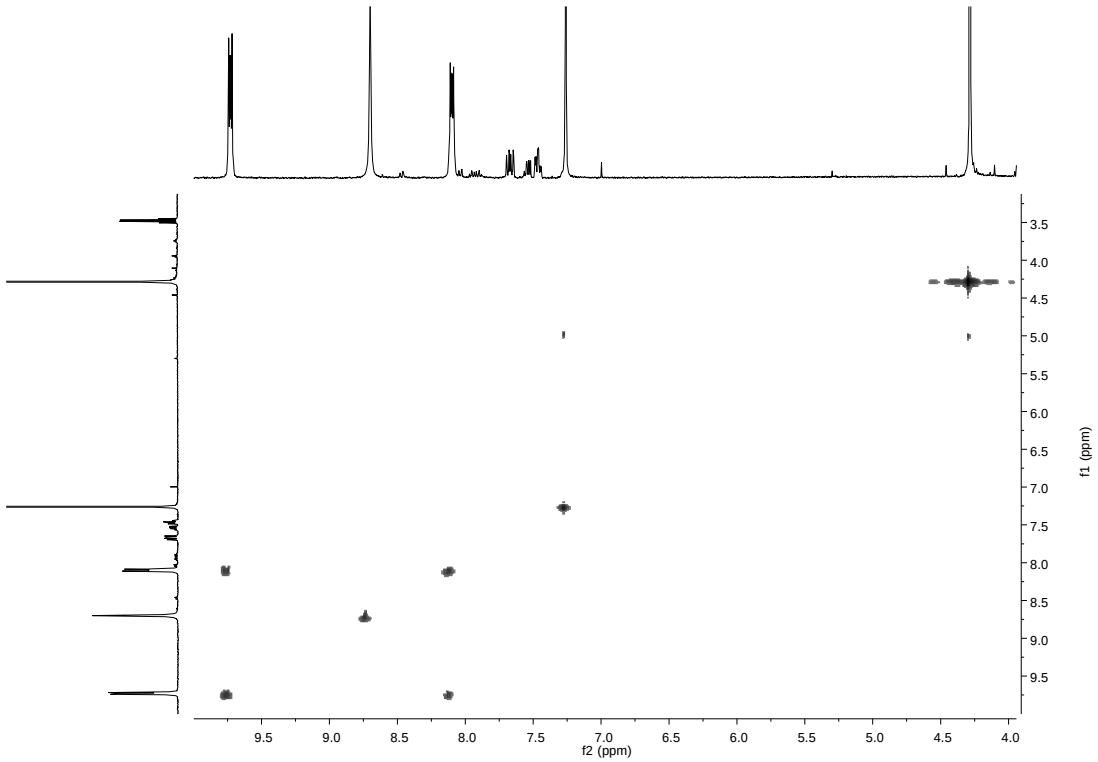

c)

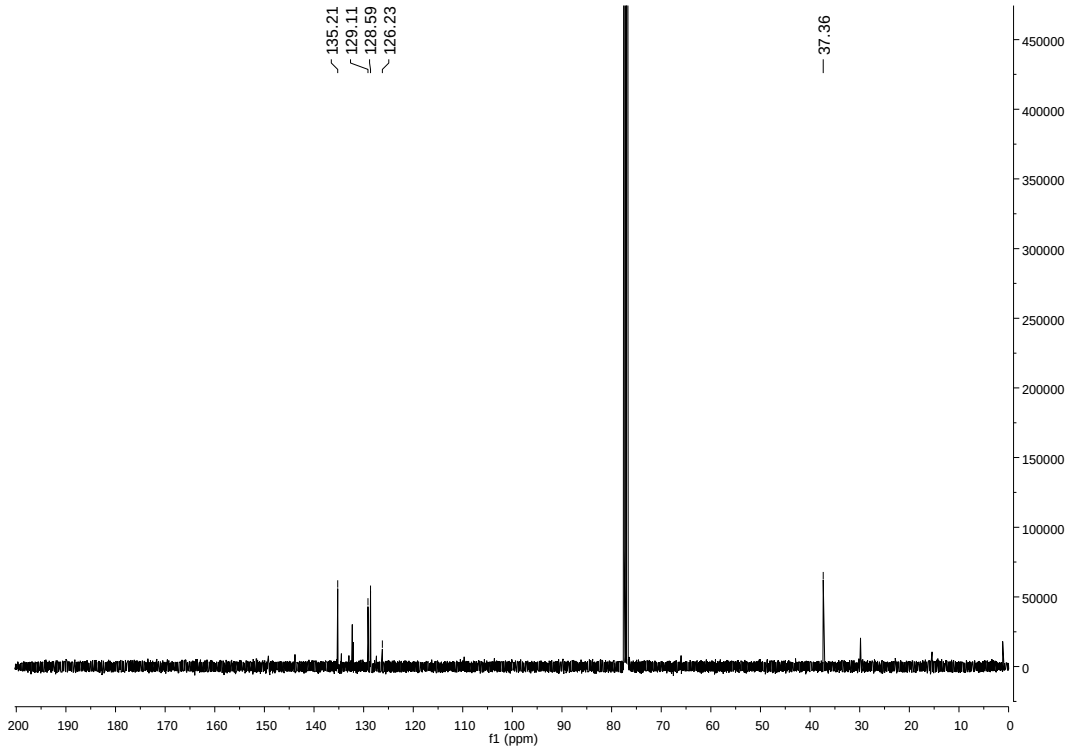

d)

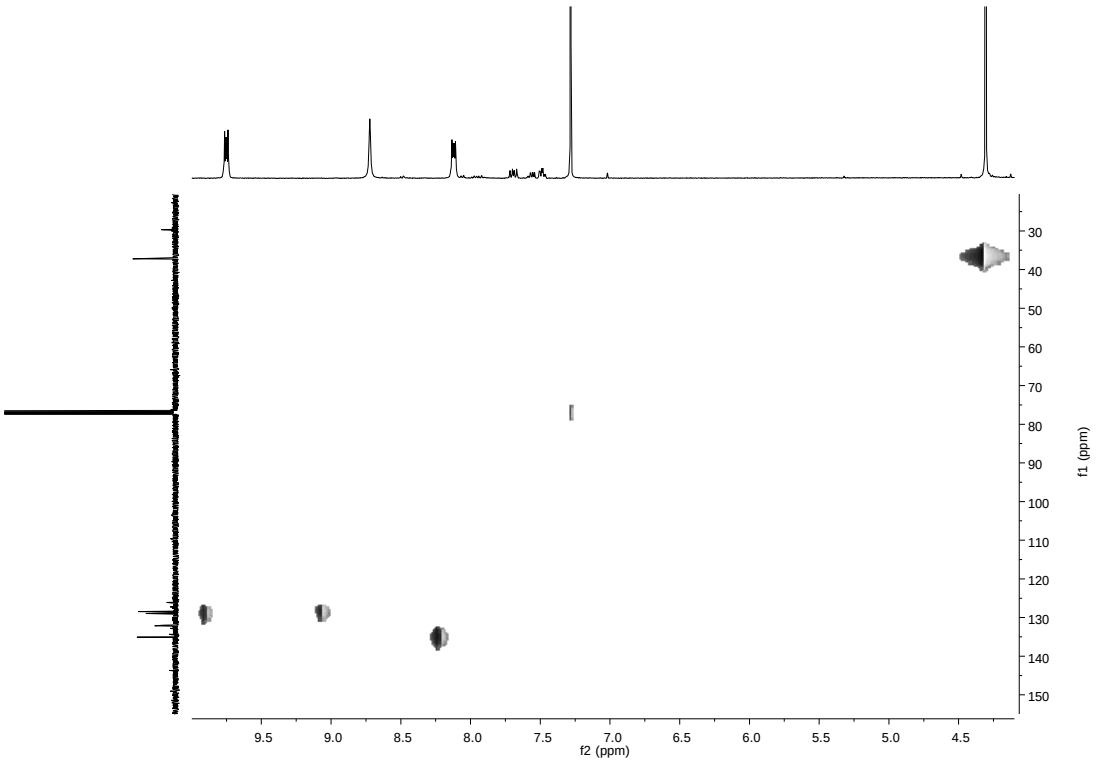

Figure S4. 1D and 2D NMR spectra (500 MHz, 298 K, $CDCl_3$) for $\mathbf{3}^{+\cdot}$. (a) $\mathbf{3}^{+}$ schematic representation and ^{1}H NMR, (b) COSY.

a)

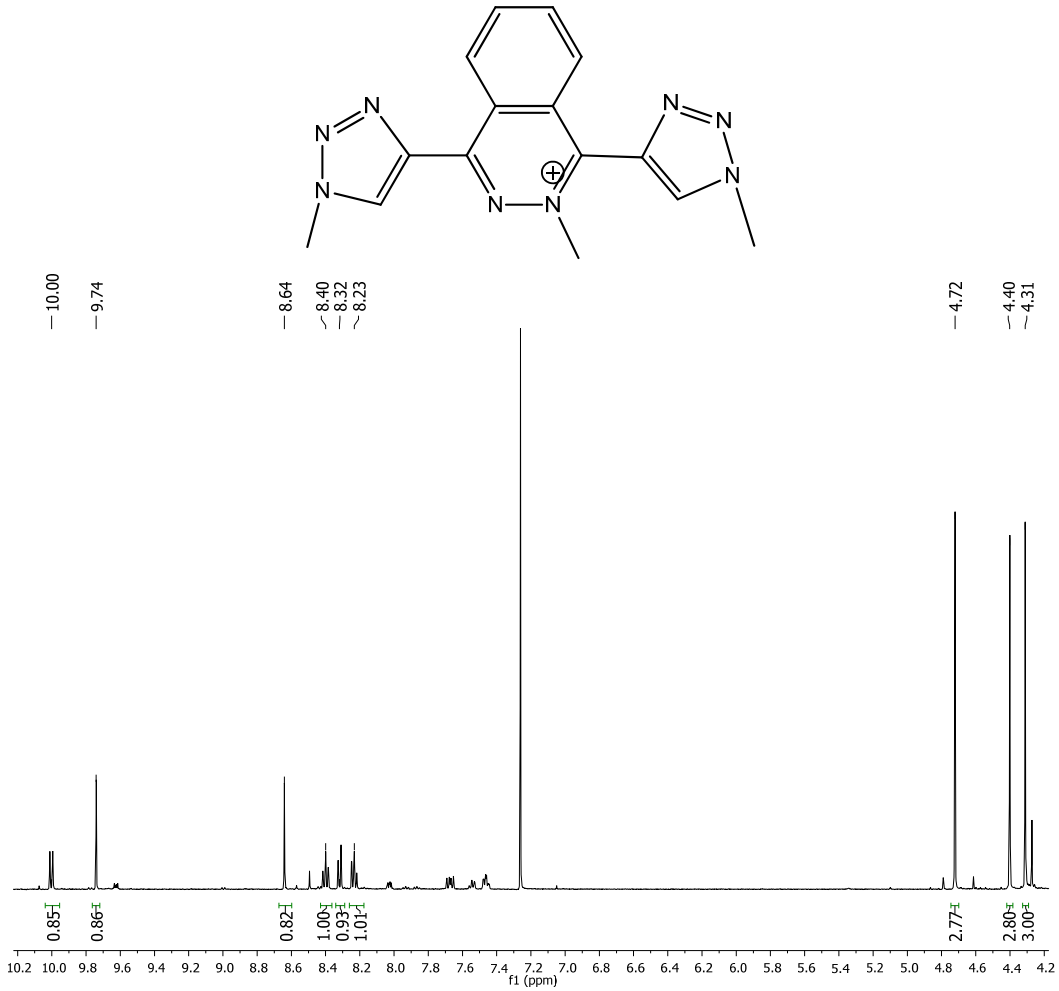

b)

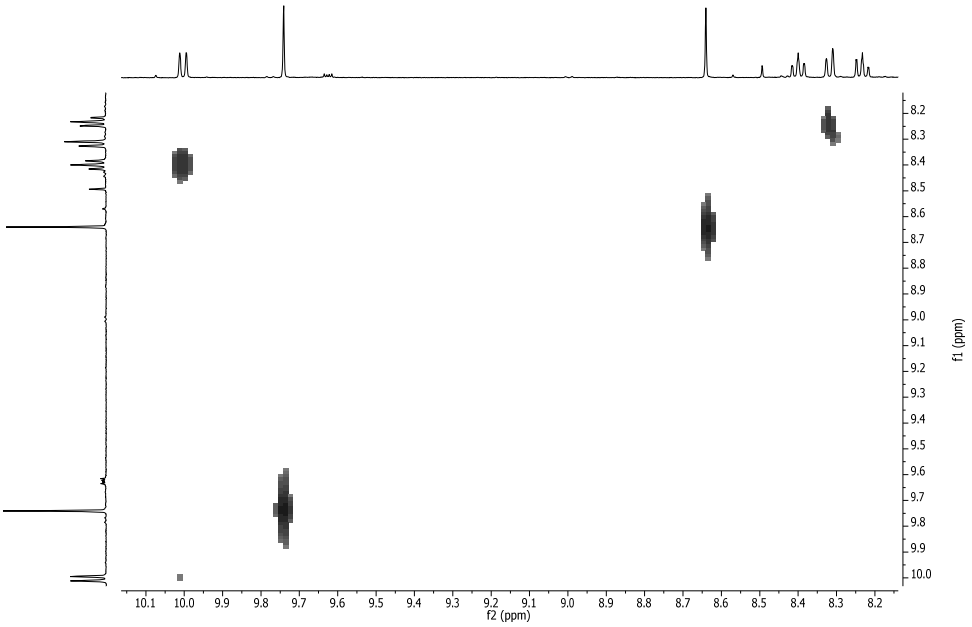

Figure S5. 1D and 2D NMR spectra (500 MHz, 298 K, CD_3CN) for $\mathbf{4}^{2+}$: (a) $\mathbf{4}^{2+}$ schematic representation and ^{1}H NMR, (b) COSY, (c) ^{13}C-{^{1}H}-NMR, (d) HSQC-NMR (aromatic region), (e) HMBC-NMR (aromatic region).

a)

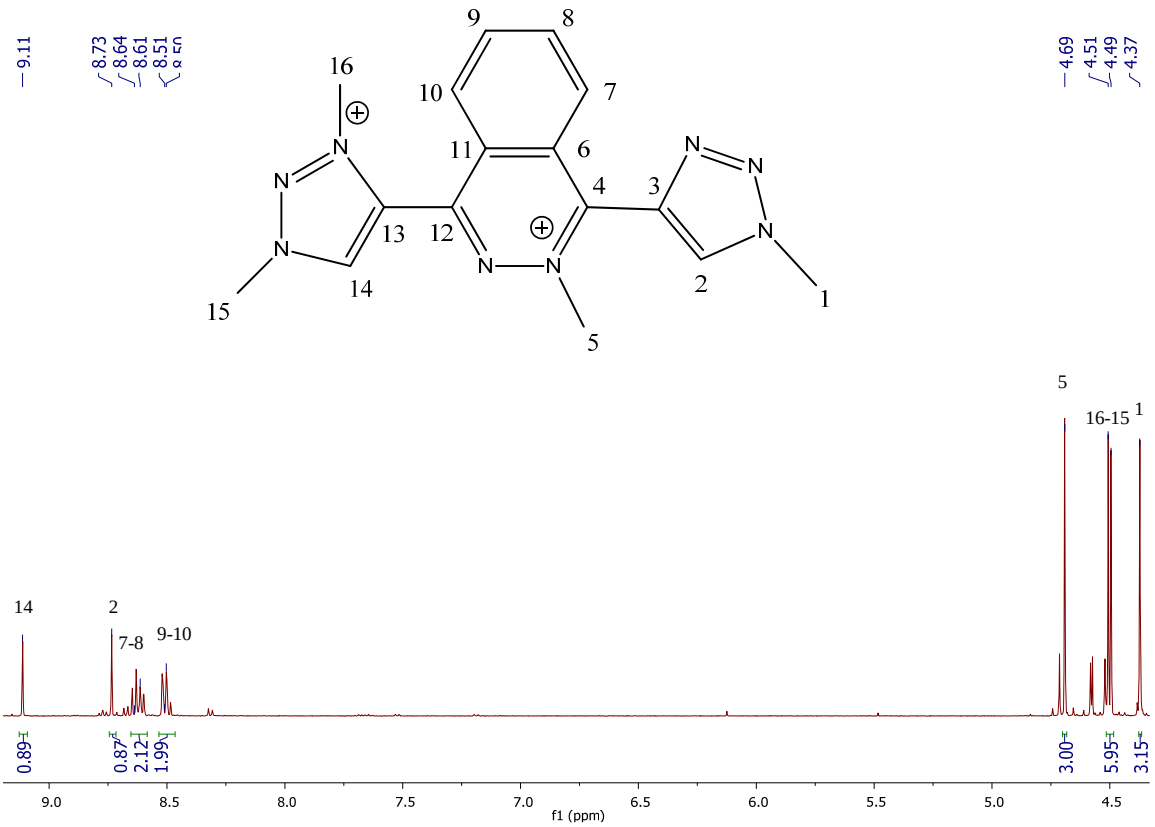

b)

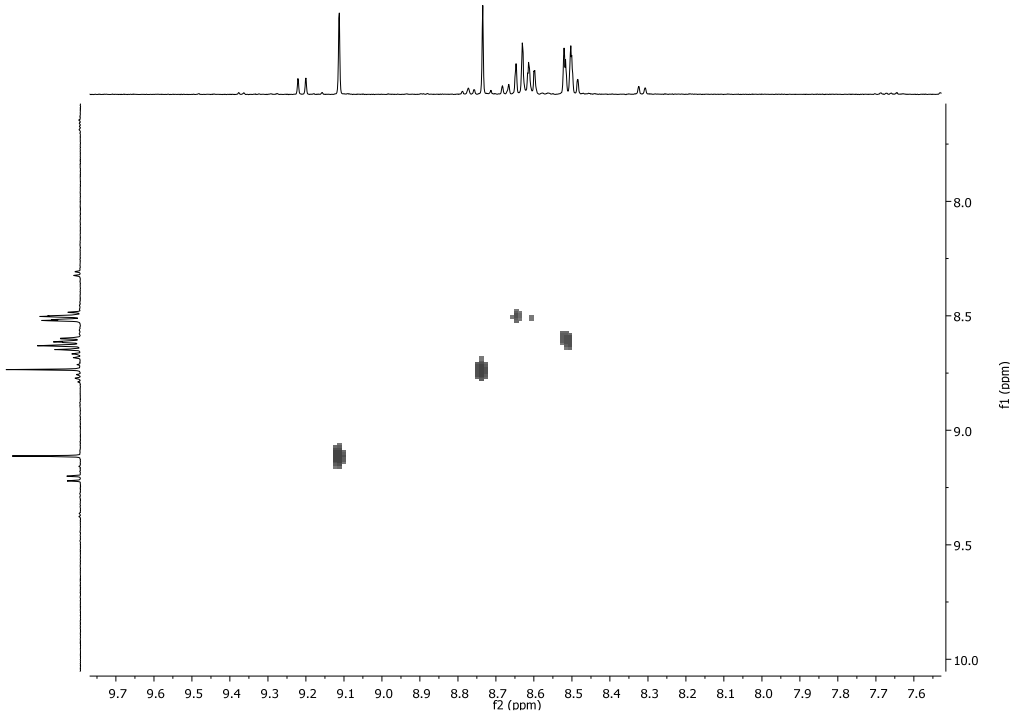

c)

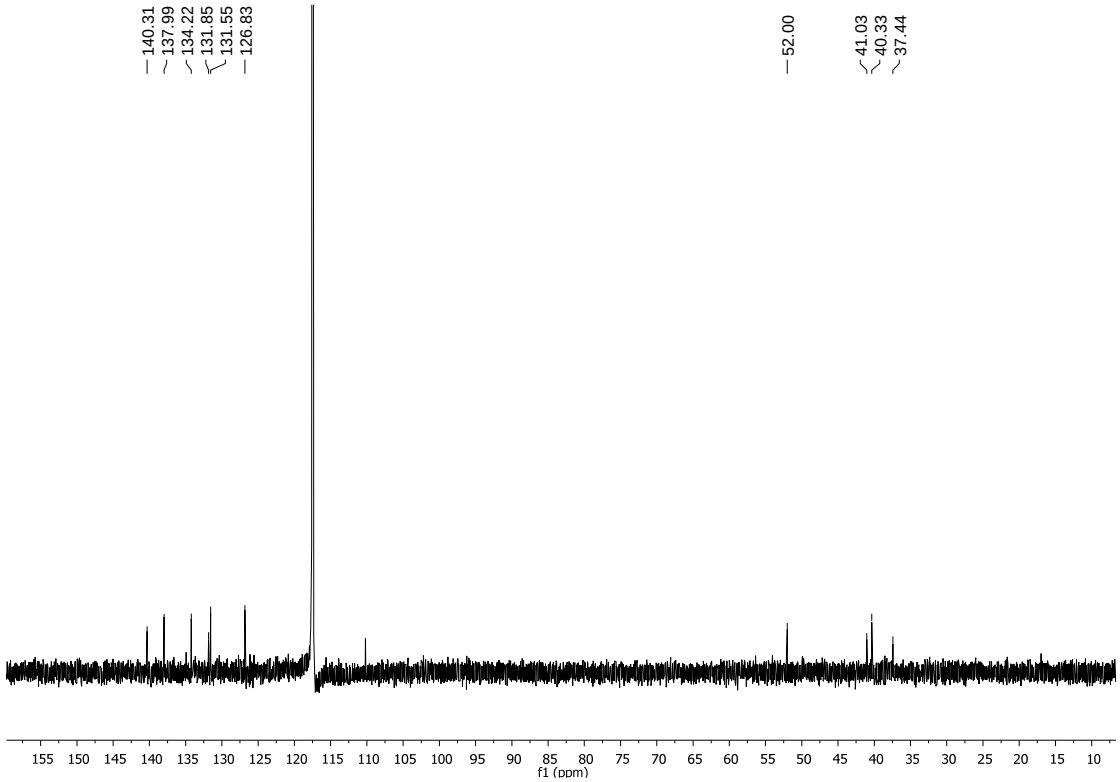

d)

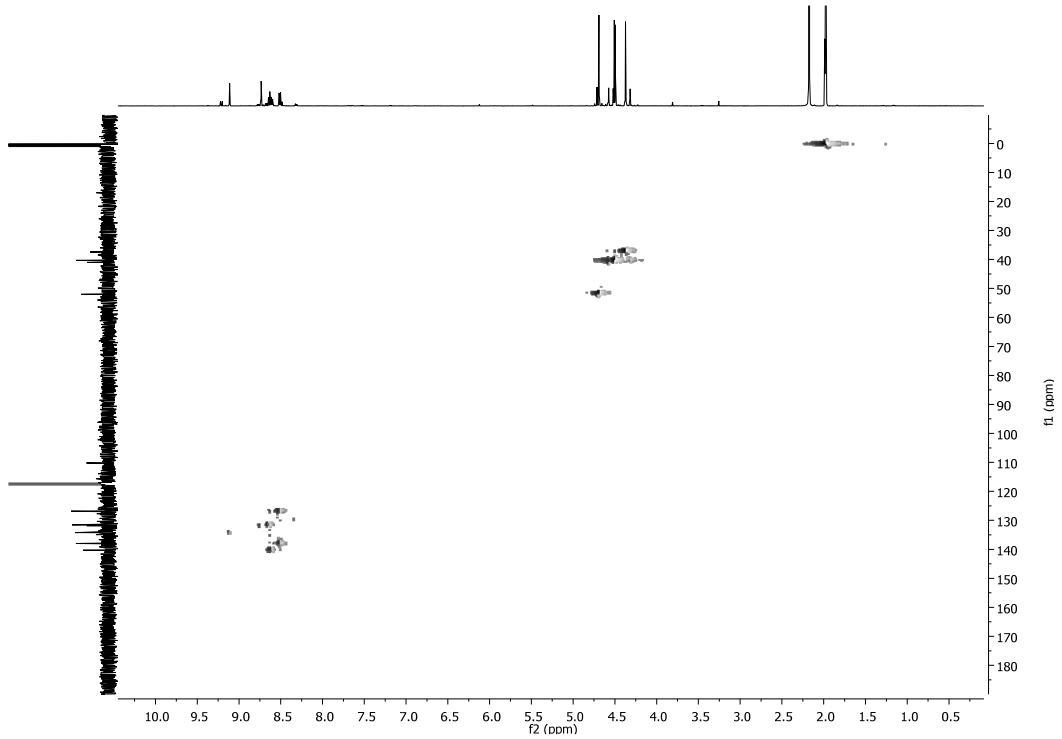

e)

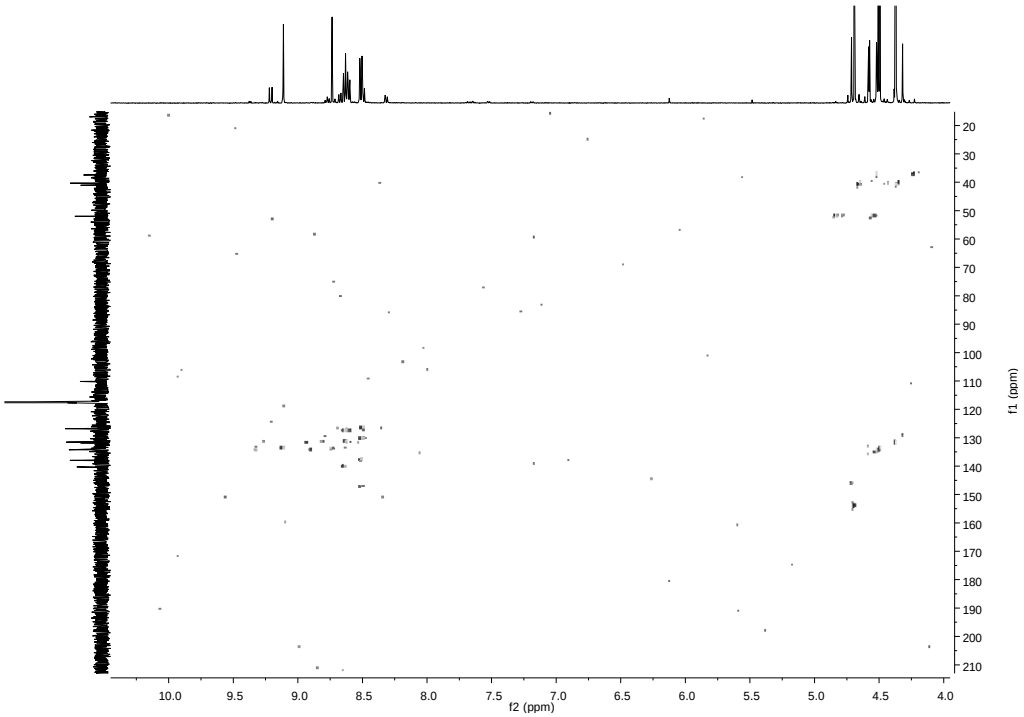

Figure S6. ^{1}H NMR spectrum (400 MHz, 298 K, acetone-d_6) recorded during the synthesis of $\mathbf{5}^{3+}$ and $\mathbf{6}^{+}$ after 12 h of reaction.

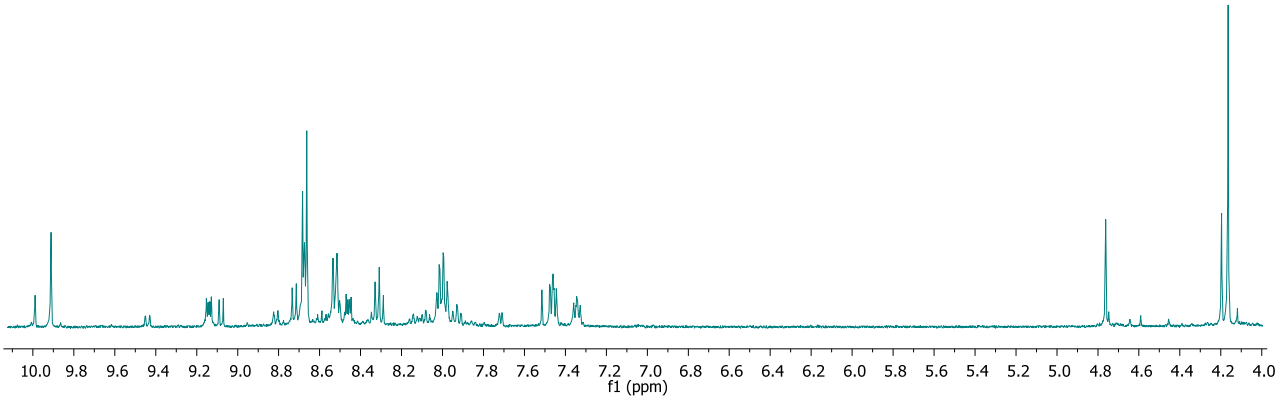

Figure S7. 1D and 2D NMR spectra (500 MHz, 298 K, acetone-d_6) for $\mathbf{5}^{3+}$: (a) $\mathbf{5}^{3+}$ schematic representation and ^{1}H NMR, (b) COSY, (c) ^{13}C-{^{1}H}-NMR, (d) HSQC-NMR (aromatic region), (e) HMBC-NMR (aromatic region).

a)

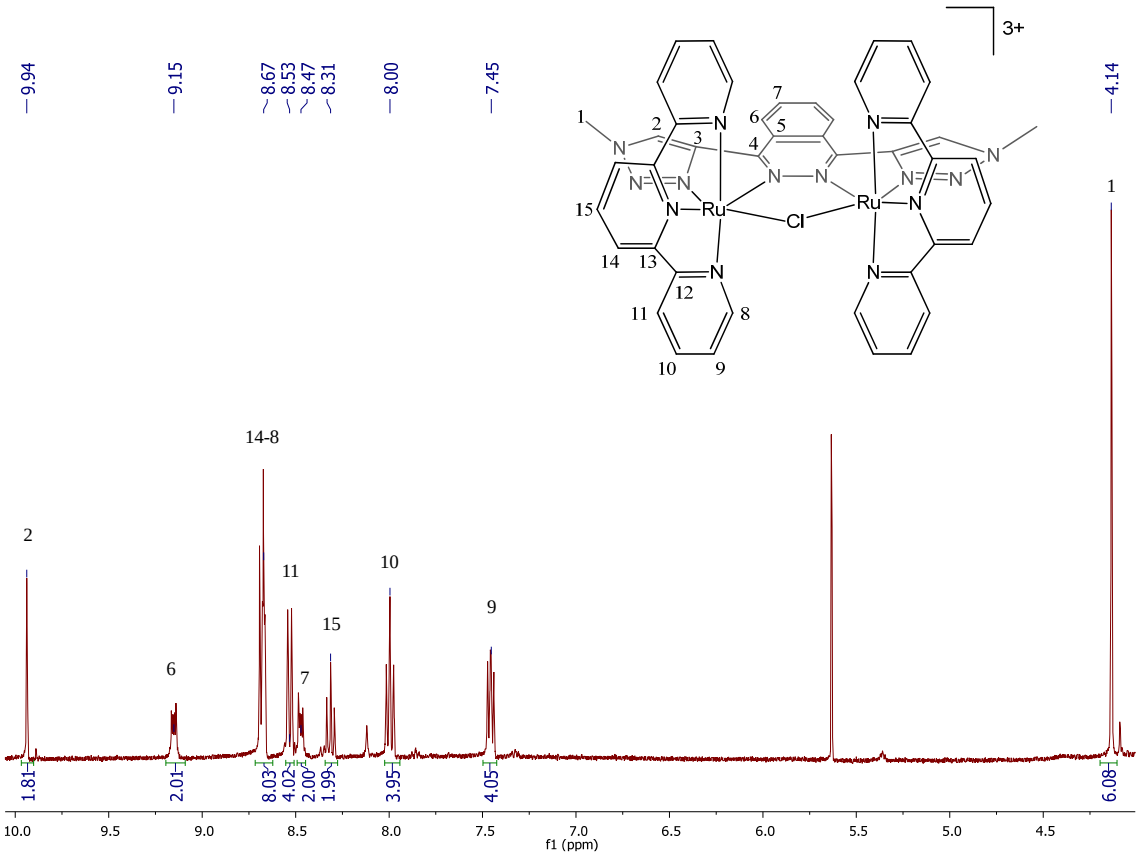

b)

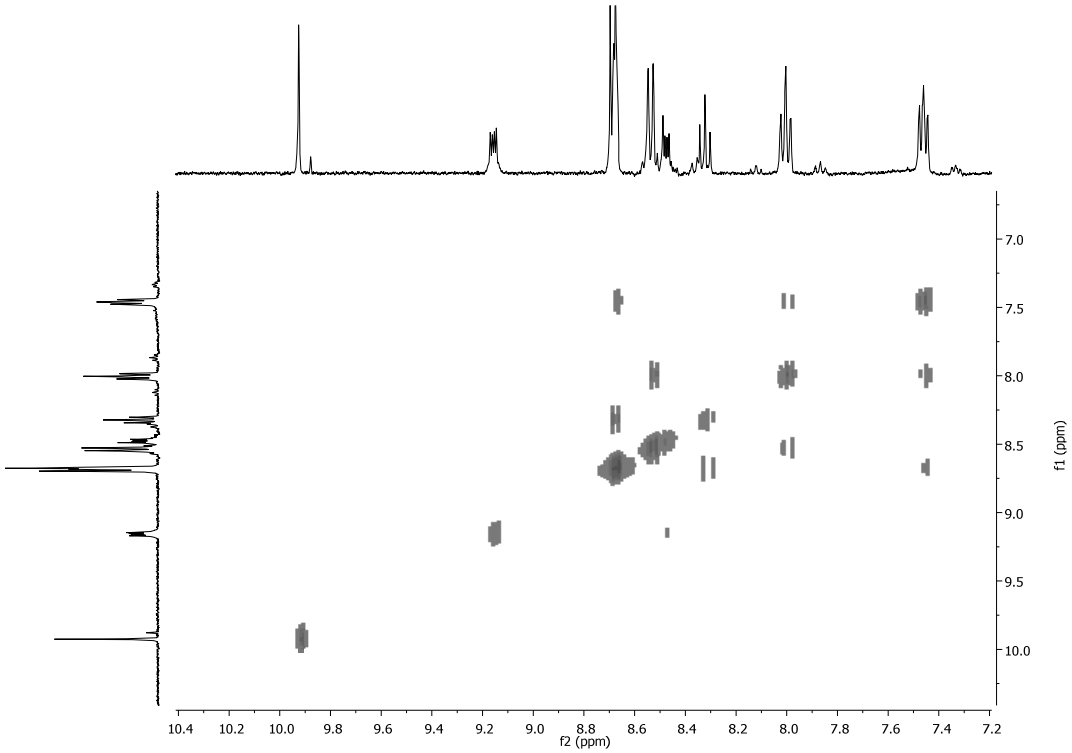

c)

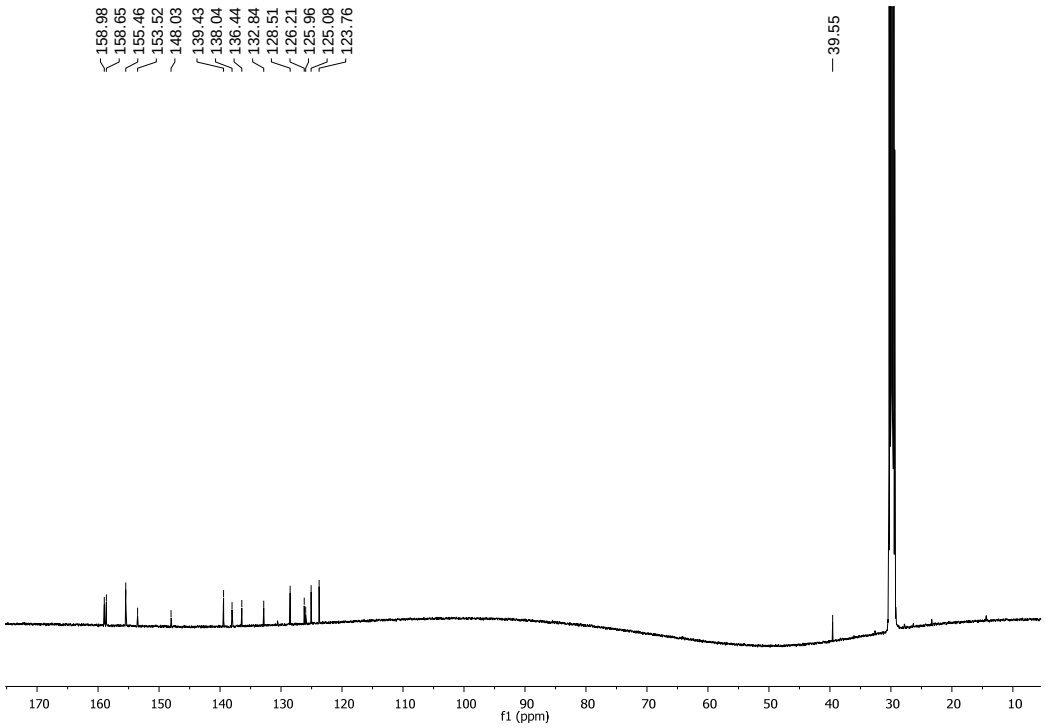

d)

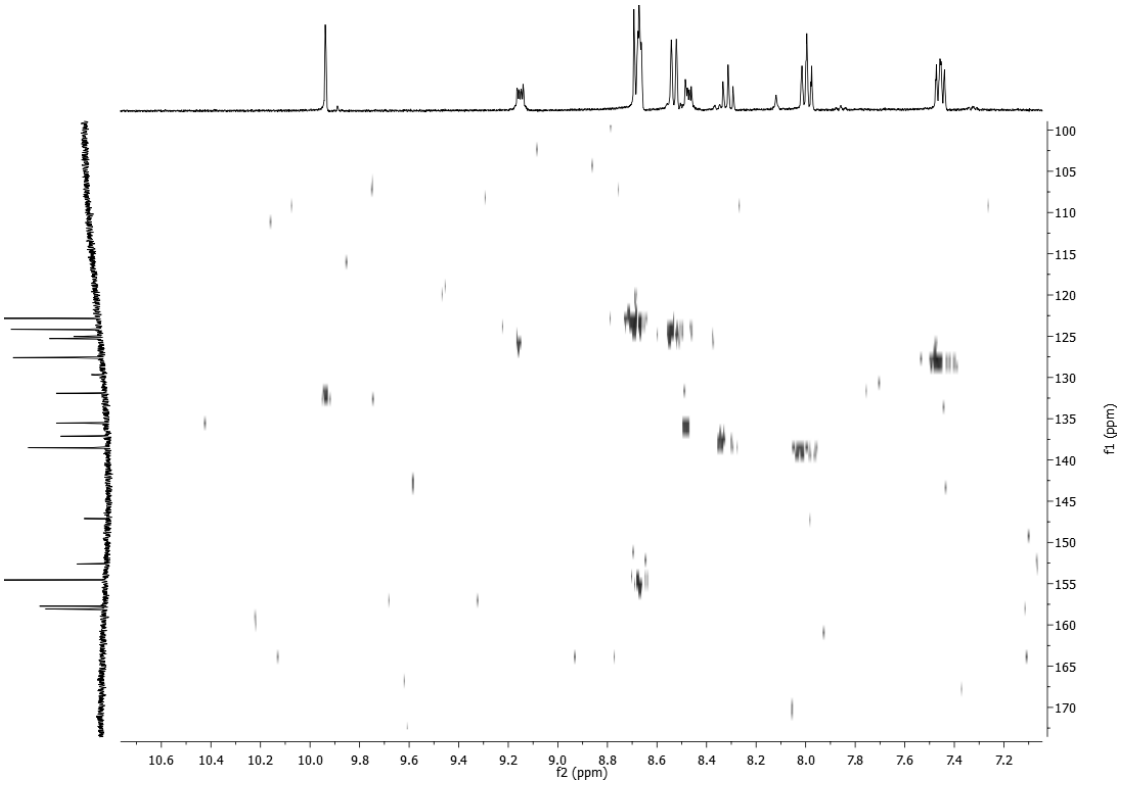

e)

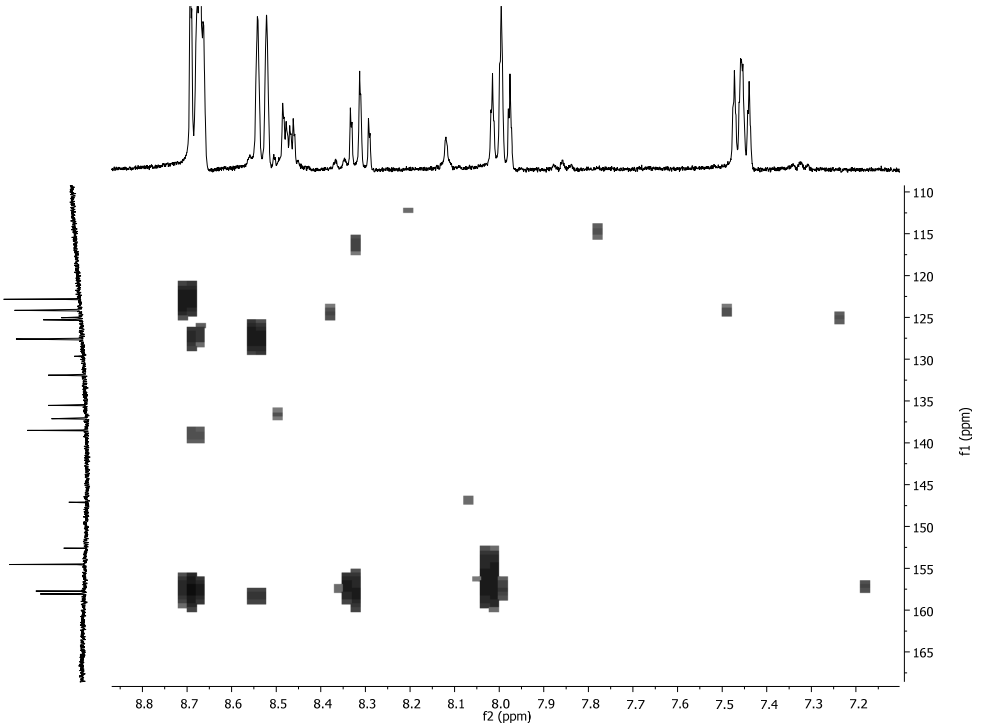

Figure S8. Schematic representation and ^{1}H NMR (400 MHz, 298 K, acetone-d_6) for **6**$^{+}$.

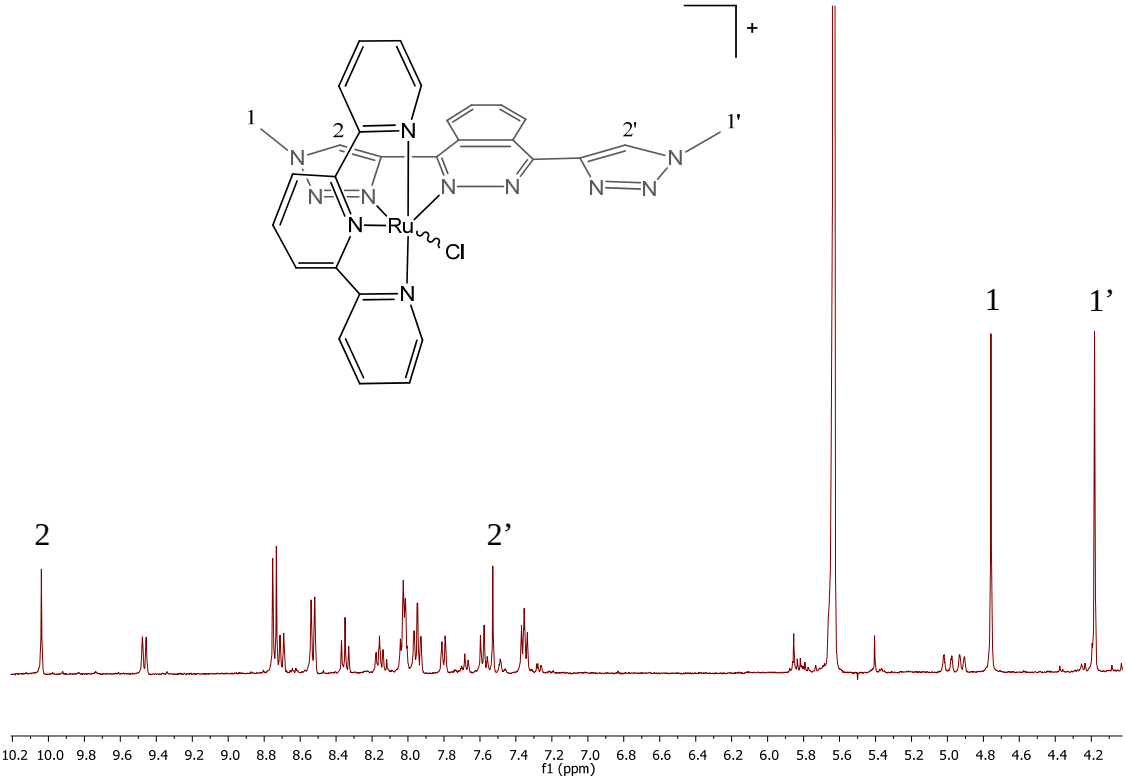

Figure S9. ESI-MS spectrum for complex $\mathbf{5}^{3+}$. Inset: theoretical (left side) and experimental (right side) isotopic distribution for peak centered at 1287.0 Da.

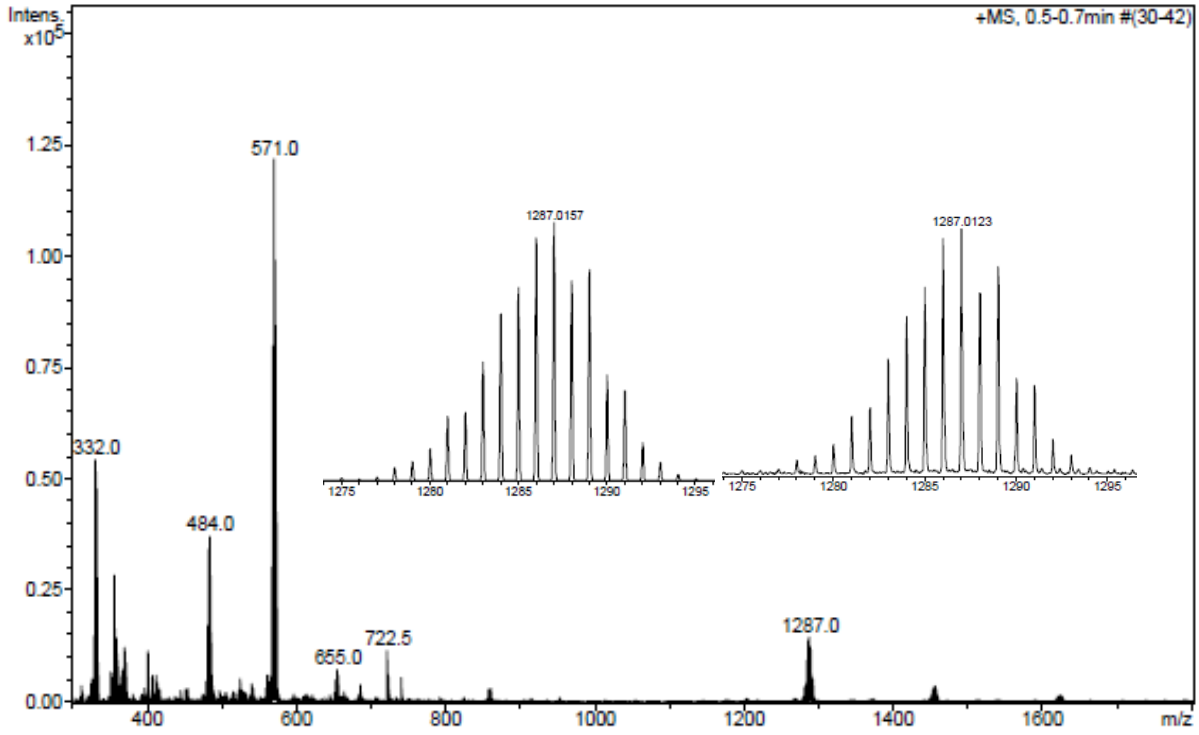

Figure S10. Cyclic voltammograms for the chlorido-bridged dinuclear complex $\mathbf{5}^{3+}$ (a) and the mononuclear complex $\mathbf{4}^{+}$ (b) in 0.1 M *n*-Bu_4NPF_6 in acetone at 100 mV/s scan rate. Glassy carbon electrode was used as working electrode and the potential was measured *vs.* SSCE.

a)

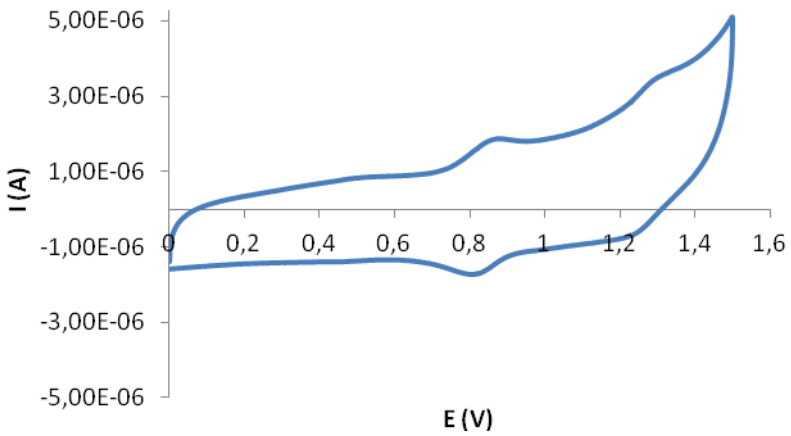

b)

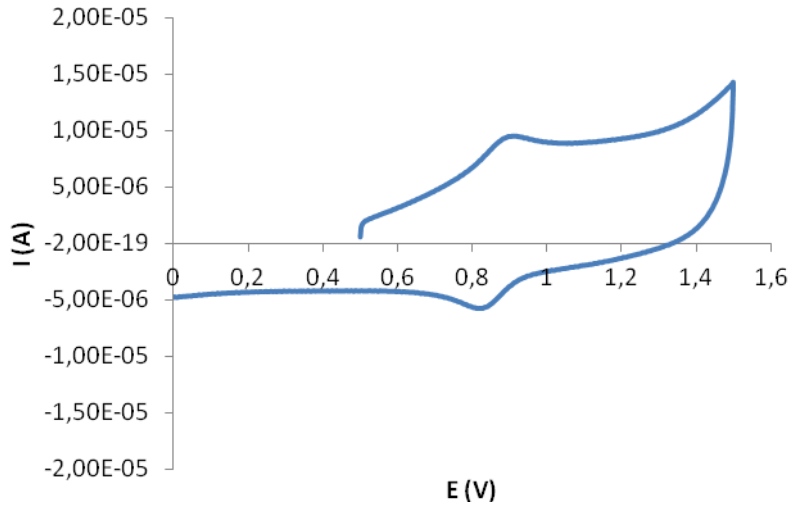

Figure S11. Mercury plot of **3(I).CHCl$_3$** unit cell.

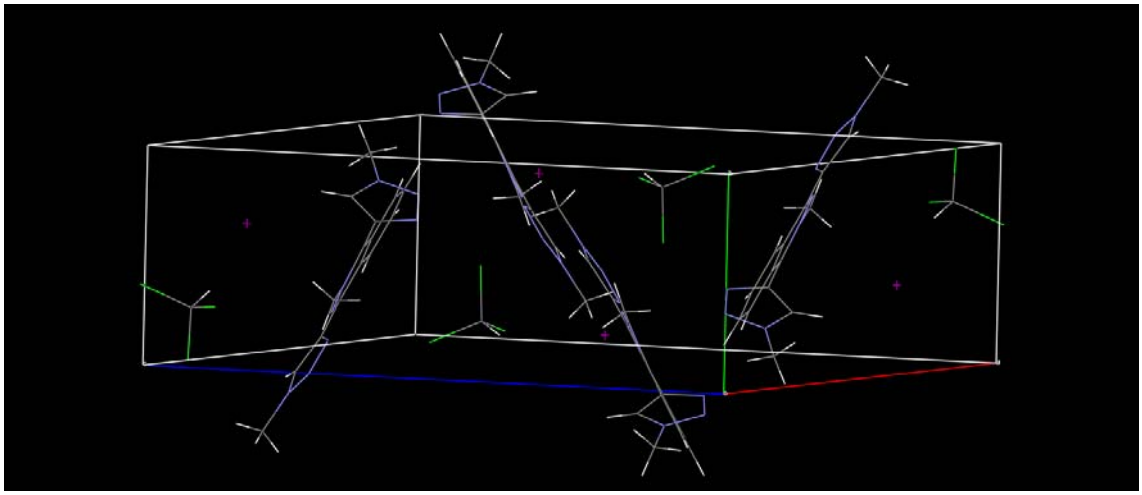

Figure S12. Mercury plot of **3**$^+$ displaying the triazole ring torsion angle.

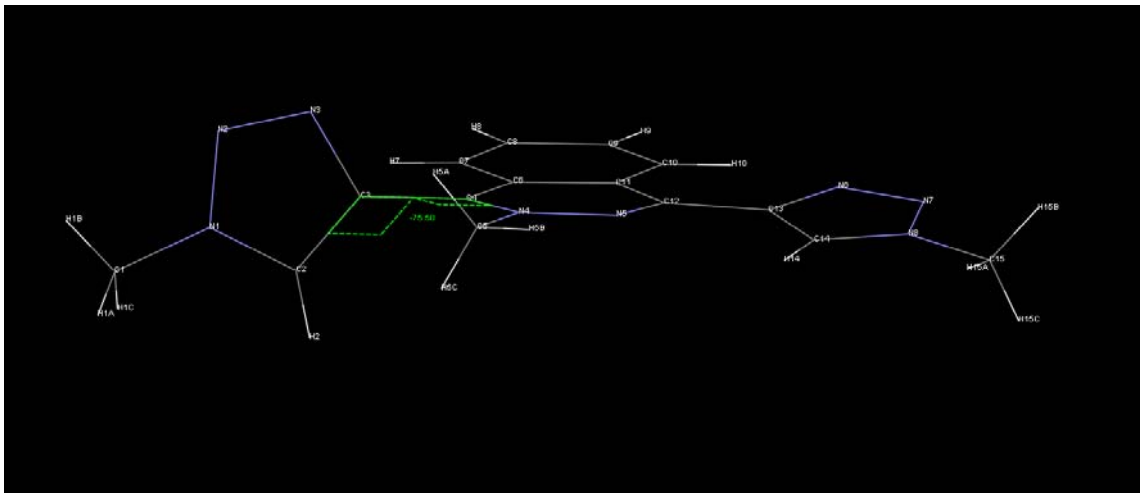

Figure S13. Mercury plot of **4**$^{2+}$ unit cell.

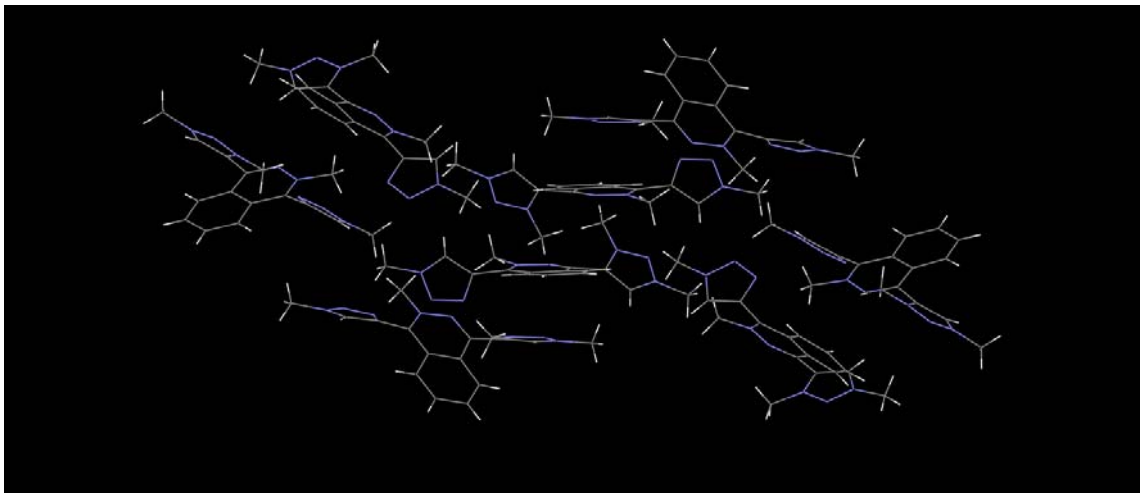

Figure S14. Mercury plot of $\mathbf{4}^{2+}$ displaying the triazole rings torsion angles.

Figure S15. Mercury plot of $\mathbf{5(PF_6)_3.2CH_3COCH_3}$ unit cell.

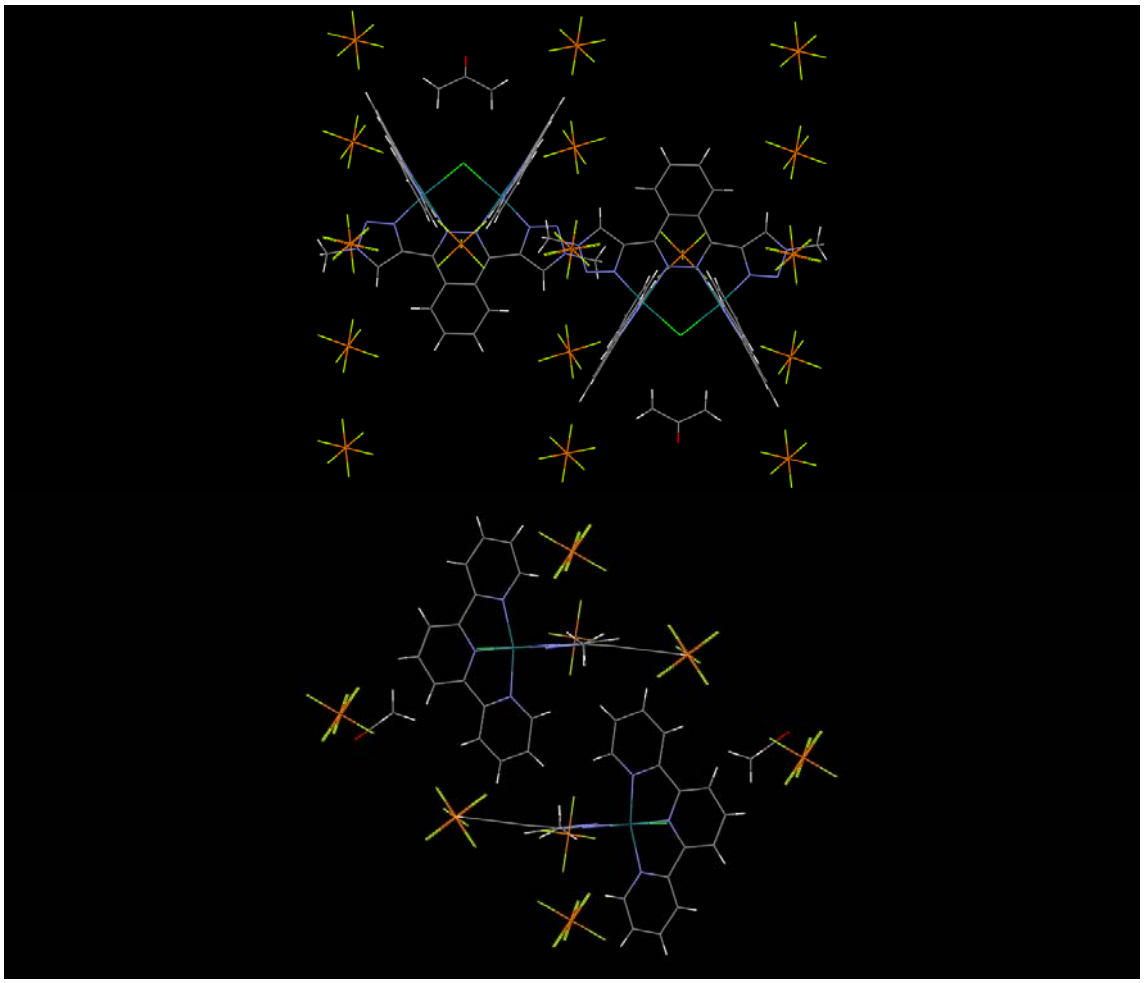

Table S1. Crystallographic data for $\mathbf{3}^{+}$.

Formula	C15 H15 N8, C H Cl3, I
Formula Weight	553.62
Crystal System	Monoclinic
Space group	P21/c (No. 14)
a, b, c [Angstrom]	16.5447(6) 6.8596(3) 19.1037(8)
V [Ang**3]	2119.32(15)
alpha, beta, gamma [deg]	90 102.175(4) 90
Z	4
D(calc) [g/cm**3]	1.735
Mu(MoKa) [/mm]	1.909
F(000)	1088
Crystal Size [mm]	0.08 x 0.10 x 0.18
Temperature (K)	100
Radiation [Angstrom]	MoKa 0.71073
Theta Min-Max [Deg]	3.3, 24.1
Dataset	-18: 18 ; -7: 7 ; -21: 21
Tot., Uniq. Data, R(int)	15714, 3351, 0.054
Observed data [I > 2.0 sigma(I)]	2791
Nref, Npar	3351, 256
R, wR2, S	0.0288, 0.0638, 1.06
w = 1/[\s^2^(Fo^2^)+(0.0197P)^2^+2.5839P] where P=(Fo^2^+2Fc^2^)/3	
Max. and Av. Shift/Error	0.00, 0.00
Min. and Max. Resd. Dens. [e/Ang^3]	-0.39, 0.79

Table S2. Crystallographic data for $\mathbf{4}^{2+}$.

Formula	C16 H18 N8, 2(C F3 O3 S)
Formula Weight	620.54
Crystal System	Orthorhombic
Space group	Pbca (No. 61)
a, b, c [Angstrom]	23.156(1) 8.0465(3) 26.901(1)
V [Ang**3]	5012.3(3)
Z	8
D(calc) [g/cm**3]	1.645
Mu(MoKa) [/mm]	0.310
F(000)	2528
Crystal Size [mm]	0.00 x 0.00 x 0.00
Temperature (K)	293
Radiation [Angstrom]	MoKa 0.71073
Theta Min-Max [Deg]	3.4, 22.0
Dataset	-24: 24 ; -8: 8 ; -28: 28
Tot., Uniq. Data, R(int)	20946, 3069, 0.056
Observed data [I > 2.0 sigma(I)]	2844
Nref, Npar	3069, 365
R, wR2, S	0.0869, 0.1660, 1.20
w = 1/[\s^2^(Fo^2^)+(0.0000P)^2^+42.4684P] where P=(Fo^2^+2Fc^2^)/	
Max. and Av. Shift/Error	0.01, 0.00
Min. and Max. Resd. Dens. [e/Ang^3]	-0.39, 0.43

Table S3. Crystallographic data for $\mathbf{5}^{3+}$.

Formula	C44 H34 Cl N14 Ru2, 3 (F6 P), 2 (C3 H6 O)
Formula Weight	1547.51
Crystal System	Monoclinic
Space group	P21/m (No. 11)
a, b, c [Angstrom]	11.8427(5) 21.0984(7) 12.933(1)
alpha, beta, gamma [deg]	90 103.303(6) 90
V [Ang**3]	3144.8(3)
Z	2
D(calc) [g/cm**3]	1.573
Mu(MoKa) [/mm]	1.573
F(000)	1480
Crystal Size [mm]	0.03 x 0.13 x 0.26
Temperature (K)	100
Radiation [Angstrom]	MoKa 0.71073
Theta Min-Max [Deg]	3.4, 24.1
Dataset	-13: 13 ; -24: 24 ; -14: 13
Tot., Uniq. Data, R(int)	14563, 5106, 0.054
Observed data [I > 2.0 sigma(I)]	3837
Nref, Npar	5106, 423
R, wR2, S	0.0485, 0.1298, 1.04
w = 1/[\s^2^(Fo^2^)+(0.0701P)^2^+1.1102P] where P=(Fo^2^+2Fc^2^)/3	
Max. and Av. Shift/Error	0.00, 0.00
Min. and Max. Resd. Dens. [e/Ang^3]	-0.52, 1.03